Temperature and Pressure Dependent Gassmann's Fluid Substitution Model for Generation of Synthetic Seismic Attributes

Yevgeniy V. Zagayevskiy and Clayton V. Deutsch

Seismic data is a valuable source of information about the architecture of a geological formation. Enhancement in 3D and 4D seismic acquisition and interpretation technology provides insight into the hidden structure of a petroleum reservoir in reservoir management decisions. Time-lapse seismic data obtained at thermally operated oil fields can help in monitoring of propagation front of hot injecting agent, for instance, in prediction of steam chamber growth in SAGD bitumen extraction method. However, the relationship between seismic attributes and reservoir temperature is not simple and further investigation is required. Also cost of conduction of repeated seismic surveys is high, and, thus, sharing seismic data with third parties is not feasible. On other hand, synthetic seismic attributes are generally accepted alternative for real data in academic community with minimal expenses. For this reason a methodology for generation of synthetic seismic attributes based on Gassmann's fluid substitution model is proposed for further use in reservoir characterization. Relationships between the attributes and reservoir pressure and temperature are considered in proposed petroelastic model. The methodology is implemented in program `fluidsub_tp.exe`*. Results are presented in the form of SAGD case study, where seismic velocities and acoustic impedances are served for estimation of geological features of a petroleum reservoir and for prediction of steam chamber growth and reservoir depletion.*

1. Introduction

Conduction of 3D seismic surveys has become a worldwide routine procedure at exploration stage of oil reserve development. 4D or time-lapse seismic surveys are employed as a reservoir management tool to a great extent (Lumley, 2001). There are several driving reasons. First, properly acquired and interpreted seismic data provide extensive spatial knowledge about reservoir. Geological characteristics of subsurface, like formation tops, faults and folds, flow barriers and baffles, can be inferred and dynamic features of a reservoir, like fluid flow, flood fronts, thief zones, can be detected by the help of geophysical advances improving reservoir management process. It has been proven that trace of injection of displacement agent in thermal oil recovery processes, such as interface between virgin reservoir zones and steam front, can be easily monitored in unconsolidated high-porosity sands by repeated seismic prospecting (Zhang et al, 2005). Secondly, the resolution of seismic data has increased recently bringing in more confidence to the data (Fahimuddin, 2010). Although availability of seismic attributes looks very promising, associated expenditures are dramatically high. Thus, service and operating companies are not willing to share data with academic community freely. This circumstance determines necessity of generation of synthetic seismic attributes for research work, which should resemble natural phenomena as close as possible to reality, but at the same time they have to be simple enough to track relation with reservoir characteristics (Hong and Deutsch, 2008).

Northern Alberta is famous for tremendous reserves of heavy oil and oil sands bitumen. Most of the reservoirs in Clearwater and McMurray formations are made of unconsolidated sandstones with high porosity. But since viscosity of deposited oil is high, such reservoirs cannot be depleted without artificial reduction of viscosity. Heavy oil can be driven out by injection of more viscous displacement agent like polymer. Even though polymer injection is relatively cheap, it is not as efficient for bitumen extraction as introduction of heat to reservoir. Steam assisted gravity drainage (SAGD) method has proven itself as a productive bitumen recovery technique and, thus, gained popularity in the industry (Butler, 1991). In SAGD several horizontal well pairs consisting of an injector and a producer are grouped together into pads covering entire area of interest. An injector is placed above a producer approximately at 5 m. High quality steam is used as a heating agent. It is injected at temperature of 200 ^{0}C or higher into a colder reservoir (on average 7 ^{0}C) through top injecting well. A steam chamber grows at constant pressure sideways and upward carrying along chamber boundaries heated and less viscous bitumen to a producing well due to gravity forces. It is obvious that heated regions and regions of a reservoir with replaced fluids in them may be detected from time-lapse seismic measurements due to change of elastic properties of effected regions, what enables monitoring of steam chamber growth and management of depletion of a reservoir.

Because of the reasons mentioned above temperature and pressure dependent petroelastic model based on Gassmann's fluid substitution model is proposed and FORTRAN program `fluidsub_tp.exe` is written for

generation of synthetic seismic attributes that are used further for SAGD process characterization. Gassmann's petroelastic model outputs seismic attributes that vary with change of fluid saturations and temperature in a reservoir, and, thus, may be used for monitoring of oil production process. Since gas is detected easier from seismic data than any other fluids (Hong et al, 2006), steam chamber growth can be predicted as well. The seismic generated by proposed model falls in class of attributes carrying low-frequency energy. They are seismic velocities of primary and secondary waves and associated acoustic impedances. Wave amplitude or attenuation rate dependent attributes are not touched in this paper.

A few papers exist in academic community, which describe generation of synthetic seismic attributes. Most of them are based on Gassmann's fluid substitution model (Gassmann, 1951; Hong et al, 2006; Mavko et al, 2009). Fahimuddin has recently implemented low frequency Gassmann theory to obtain seismic data in order to characterize reservoir by means of modeling technique Ensemble Kalman Filter (Fahimuddin, 2010). Equations for relationship between acoustic properties of saturated rock and reservoir pressure and temperature can be found in the paper by (Batzle and Wang, 1992). MATLAB implementation framework of Gassmann's fluid substitution model is documented in the paper by (Kumar, 2006). Proposed methodology for generation of temperature and pressure dependent seismic attributes is summary work of mentioned papers. Associated program `fluidsub_tp.exe` has some similarities with program `fluidSub.exe` by (Hong and Deutsch, 2008). However, it differs from its predecessor in taking into account non-isothermal environment for acoustic wave propagation, i.e. in new program elastic and physical properties of fluids and saturated rock are expressed as a function of thermodynamic state of reservoir. Assumption is made regarding temperature insensitive properties of constituent minerals.

This paper is organized in following manner. First of all, importance of 4D seismic data acquisition contrary to 3D seismic surveys is discussed. Second, theoretical background of Gassmann's fluid substitution model is presented along with relationship between acoustic properties of saturated rock and fluids and thermo physical properties of reservoir (temperature and pressure). Fluid components are divided into three main groups (brine water, oil, and gas) and are studied separately. Third, description of parameter file of FORTRAN program `fluidsub_tp.exe` is given. Porosity, fluid saturations, mineralogical content of a rock, elastic and physical properties of constituents should be specified and synthetic P- and S-wave velocities and associated acoustic impedances for volumetric model are generated by the program. Four, SAGD case study is presented, where the seismic is used to characterize reservoir heterogeneity, and difference between baseline seismic survey and subsequent repeated surveys is employed to monitor steam chamber growth and to detect flow barriers. Finally, conclusion regarding proposed petroelastic model is made as well. Appendix is attached as well, where a description of two auxiliary FORTRAN programs is given. The program `starstogslib.exe` converts output of CMG's thermal flow simulator STARS to GSLib (Geo_EAS-like) format. The program `seisdif.exe` computes difference between seismic attributes from baseline survey and all subsequent repeated surveys.

2. Necessity of 4D Seismic Surveys

Acoustic waves are energy waves that transport energy through an elastic medium in patches. Seismic waves are a type of low frequency acoustic waves, where propagation occurs through the Earth or its surface. Thus, seismic waves may be either surface waves or body waves, latter ones being of greater interest. The surface waves propagate along surface of the Earth. The body waves occur through inner part of the Earth. They can be divided into two groups: longitudinal or compressional primary (P-) waves and transverse or shear secondary (S-) waves. In longitudinal waves vibration occurs parallel to direction of wave travel, in transverse waves – perpendicular to direction of wave travel. P-waves are called primary because their propagation speed is faster than propagation speed of S-waves, and, therefore, they are detected first by receivers. The propagation velocity is a function of density and elastic properties of a medium (bulk and shear moduli, Poisson's ratio, etc.). It is possible to distinguish between properties of rocks and later to differentiate rock types by measuring wide range of seismic waves coming from interior of the Earth at different velocities.

While natural source of seismic waves are earthquakes, they also can be artificially generated by explosion or dropping heavy objects to a surface. Seismic data are acquired, processed, interpreted and analyzed to extract important information about geological architecture of subsurface. Any information extracted from records of seismic waves, for instance, travel time of a wave between source and detector, difference in amplitude or frequency of a wave at source and receiver, energy attenuation rate, is called a seismic attribute.

4D seismic surveys are set of repeated 3D or 2D seismic surveys over calendar time. While first three dimensions are aimed to characterize acoustic properties of saturated rock in space, fourth dimension captures time. The main advantage of 4D seismic surveys over 3D is that hardly recognized combined acoustic properties of rock and fluids can be separated in time-lapse seismic data, and, thus, fluid flow can be predicted and managed. Even though rock properties may change in time due to human invasion into reservoir, their variation is assumed to be negligible in time. On the other hand because fluid flows through reservoir during period of oil production, changes in fluid saturations are reflected in seismic data. Simple subtraction of baseline seismic survey, which is conducted at exploration stage prior to production, from repetitive seismic readings enables to eliminate impact of geology on seismic data, and, thus, to retain only dynamic component associated with fluid flow. It is important for time increment in 4D seismic acquisition to be long enough to track changes of fluid saturations. Therefore, on average 4D seismic survey is conducted every one or two years. The frequency of repetition is also limited by a company budget. The proposed Gassmann model may be used to quantify benefit of 4D seismic surveys and to estimate repetition frequency based on derived uncertainties.

3. Gassmann's Fluid Substitution Model

Synthetic seismic attributes should be a function of elastic and physical properties of fluids and rock and reservoir pressure and temperature in order to define reservoir architecture and monitor flow of injected heating agent in thermally operated oil extraction processes. Any change in fluid composition and temperature should be reflected in repeated synthetic seismic attributes. Also noise should be incorporated into synthetic attributes to resemble the complexity associated with acquisition of real seismic data. In this methodology it is assumed that artificial noise follow normal distribution with zero mean and specified standard deviation in percentage of pure seismic value.

Among wide diversity of seismic attributes P- and S-wave velocities and corresponding acoustic impedances (V_P, V_S, Z_P, and Z_S) are chosen and derived from Gassmann's fluid substitution model, because of their ability to detect change in fluid saturations and reservoir temperature. Workflow of derivation of pressure and temperature dependent seismic velocities and acoustic impedances is schematically presented in the Figure 4. Mathematical elaboration is explained below as well.

Relationship between seismic velocity and acoustic impedance can be expressed as follows:

$$Z_P = \rho_{sat} \cdot V_P \tag{1}$$

$$Z_S = \rho_{sat} \cdot V_S \tag{2}$$

where, V_P and V_S are the P- and S-wave seismic velocities, m/s; Z_P and Z_S are the P- and S-wave characteristic acoustic impedances, Pa*s/m; ρ_{sat} is the density of saturated rock (rock with pore fluid, which can be brine water, oil, gas, or their mixture), kg/m^3.

Seismic velocities in isotropic, homogenous, elastic medium can be computed as shown in Equations (3) and (4).

$$V_P = \sqrt{\frac{K_{sat} + \frac{4}{3}\mu_{sat}}{\rho_{sat}}} \tag{3}$$

$$V_S = \sqrt{\frac{\mu_{sat}}{\rho_{sat}}} \tag{4}$$

where, K_{sat} is the effective elastic bulk modulus of saturated rock, Pa; μ_{sat} is the effective elastic shear modulus of saturated rock, Pa.

Bulk and shear moduli of saturated rock can be computed from low-frequency Gassmann theory:

$$\frac{K_{sat}}{K_{matrix}-K_{sat}}=\frac{K_{dry}}{K_{matrix}-K_{dry}}+\frac{K_{fluid}}{\phi\cdot(K_{matrix}-K_{fluid})} \tag{5}$$

$$\mu_{sat}=\mu_{dry} \tag{6}$$

where, K_{dry} and μ_{dry} are the effective elastic bulk and shear moduli of dry rock (no presence of pore fluid), Pa; K_{matrix} is the bulk modulus of the mineral material of the rock, Pa; φ is the porosity of the rock medium.

Bulk modulus of dry rock is derived from laboratory measurements, empirical relationship, or wireline log data, and can be approximately described as follows:

$$K_{dry}=K_{matrix}(1-\beta) \tag{7}$$

$$\mu_{dry}=\mu_{matrix}(1-\beta) \tag{8}$$

where, β is the Biot coefficient defined as the ratio of pore-volume change Δv_p to bulk-volume change ΔV at constant pore pressure.

Empirical equation of Biot coefficient can be presented as follows (Krief et al, 1990):

$$(1-\beta)=(1-\phi)^{\frac{3}{1-\phi}} \tag{9}$$

Since it is intended to apply synthetic seismic attributes for characterization of Northern Alberta oil fields, lithology of a reservoir can be approximated to local formations. Thus, lithofacies of McMurray formation can be represented by several classes. Frequently encountered facies are sand, shale, sandy and muddy IHS, breccia, mudstone, and carbonate. Most of them comprise two distinct lithological sequences: permeable sand and impermeable shale. Their presence in facies is expressed through volume fraction coefficient called *V*-shale, which is the ratio of rock volume occupied by shale to total volume of rock specimen (*V*-shale = V_{shale}/V_{total}). Hence, lithology of any facies can be simply described by shale content, where *V*-shale value determines volume of shale and (*1* – *V*-shale) determines volume of sand in a facies. Mineralogy of these two sequences mainly consists of two minerals: quartz and clay. While quartz is more dominant in sand, shale is mostly made of clay particles. On average it can be assumed that volume fraction of quartz f_{quartz} is 0.3 and f_{clay} is 0.7 ($f_{clay}+f_{quartz}=1.0$). Described mineralogical model provides grounds for calculation of elastic moduli and density of rock matrix.

Bulk and shear moduli of rock matrix can be approximated by average of Hashin-Shtrikman bounds for isotropic linear elastic composite consisting of only two constituent minerals (Equations (10) and (11)).

$$K_{matrix}=\frac{K_{matrix}^{upperHS}+K_{matrix}^{lowerHS}}{2} \tag{10}$$

$$\mu_{matrix}=\frac{\mu_{matrix}^{upperHS}+\mu_{matrix}^{lowerHS}}{2} \tag{11}$$

$$K_{matrix}^{upperHS/lowerHS}=K_{1/2}+\frac{f_{2/1}}{(K_{2/1}-K_{1/2})^{-1}+f_{1/2}\cdot\left(K_{1/2}+\frac{4}{3}\mu_{1/2}\right)^{-1}} \tag{12}$$

$$\mu_{matrix}^{upperHS/lowerHS}=\mu_{1/2}+\frac{f_{2/1}}{(\mu_{2/1}-\mu_{1/2})^{-1}+2\cdot f_{1/2}\cdot\frac{(K_{1/2}+2\cdot\mu_{1/2})}{5\cdot\mu_{1/2}\cdot\left(K_{1/2}+\frac{4}{3}\mu_{1/2}\right)}} \tag{13}$$

where, $K^{upperHS}_{matrix}$ and $K^{lowerHS}_{matrix}$ are the upper and lower Hashin-Shtrikman bounds for bulk modulus of two constituent isotropic elastic medium, Pa; $\mu^{upperHS}_{matrix}$ and $\mu^{lowerHS}_{matrix}$ are the upper and lower Hashin-Shtrikman bounds for shear modulus, Pa; K_1 and K_2 are the bulk moduli of individual constituents (quartz and clay), Pa; μ_1 and μ_2 are the shear moduli of individual constituents, Pa; and f_1 and f_2 are the volume fractions of individual minerals; slash separates order of constituents in calculation of upper and lower bounds.

It has been mentioned that fluid component of a reservoir may be represented as a single brine water, oil, and gas or various mixture of them. Thus, fluid bulk modulus K_{fluid} can be derived using Reuss (isostress) average of fluid mixture taking into account bulk modulus of every fluid type:

$$\frac{1}{K_{fluid}} = \frac{S_{brine}}{K_{brine}} + \frac{S_{oil}}{K_{oil}} + \frac{S_{gas}}{K_{gas}} \tag{14}$$

where, K_{brine}, K_{oil} and K_{gas} are the bulk modulus of brine water, oil, and gas respectively, Pa; S_{brine}, S_{oil} and S_{gas} are the brine water, oil, and gas saturations respectively, they have to sum up to 1.0 ($S_{brine} + S_{oil} + S_{gas} = 1.0$).

Density of saturated rock can be expressed as follows:

$$\rho_{sat} = (1-\phi)\cdot\rho_{matrix} + \phi\cdot\rho_{fluid} \tag{15}$$

where, ρ_{matrix} and ρ_{fluid} are the densities of rock matrix and fluid mixture of brine water, oil, and gas respectively, kg/m^3.

Density of fluid mixture is

$$\rho_{fluid} = S_{brine}\cdot\rho_{brine} + S_{oil}\cdot\rho_{oil} + S_{gas}\cdot\rho_{gas} \tag{16}$$

where, ρ_{brine}, ρ_{oil} and ρ_{gas} are the densities of brine water, oil, and gas at reservoir pressure and temperature respectively, kg/m^3.

Matrix density can be also expressed through density and volume fraction of quartz and clay minerals:

$$\rho_{matrix} = f_{clay}\cdot\rho_{clay} + f_{quartz}\cdot\rho_{quartz} \tag{17}$$

Relationship between elastic properties and densities of fluids and temperature and pressure are summarized in next sections for every fluid component. It is assumed that properties of rock are independent of temperature or pressure, and, therefore, are constant. Elastic and seismic properties of quartz and clay are summarized in the Table 1. Same properties of fluid components are presented in the Table 2. Note that transverse waves cannot be generated in liquid or gas phases.

Table 1: Elastic and seismic properties of clay and quartz minerals

Mineral	Density (g/cm^3)	Bulk modulus (GPa)	Shear modulus (GPa)	V_p (km/s)	V_s (km/s)
Clay (kaolinite)	1.58	15.0	6.0	1.44	0.93
Quartz	2.65	37.0	44.0	6.05	4.09

Table 2: Elastic and seismic properties of pure water, heavy oil (bitumen) and natural gas at standard conditions (15.6 ^{0}C, 0.1 MPa)

Fluid	Density (g/cm^3)	Bulk modulus (GPa)	V_p (km/s)
Pure water	0.9991	2.20	1.497
Heavy oil	1.0100	1.66	1.500
Natural gas	0.0008	0.01	0.450

a) Brine water

Bulk modulus for homogeneous liquid or gas can be expressed through Newton-Laplace equation:

$$V = \sqrt{\frac{K}{\rho}} \tag{18}$$

where, V is the P-wave sound velocity in a homogeneous liquid or gaseous medium, m/s; K is the bulk modulus of the medium, Pa; ρ is the density of the medium, kg/m^3.

Bulk modulus can be easily found from the Equation (18), when density and acoustic velocity of homogeneous liquid or gas substance are known at specific pressure and temperature. Thus, Equation (19) is used to compute bulk moduli of brine water, oil, and gas.

$$K = \rho \cdot V^2 \tag{19}$$

It has been derived empirically that acoustic velocity of brine water free of gas can be approximately expressed as:

$$\begin{aligned} V_{brine} &= V_{water} + \chi \cdot (1170 - 9.6 \cdot T + 0.055 \cdot T^2 \\ &- 8.5 \times 10^{-5} T^3 + 2.6 \cdot P - 0.0029 \cdot T \cdot P - 0.0476 \cdot P^2) \\ &+ \chi^{1.5} \cdot (780 - 10 \cdot P + 0.16 \cdot P^2) - 820 \cdot \chi^2 \end{aligned} \tag{20}$$

where, V_{brine} is the acoustic velocity in brine water, m/s; V_{water} is the acoustic velocity in fresh water, m/s; P and T are the pressure and temperature of brine water, MPa and ^{0}C; χ is the salinity of brine water or weight fraction of dissolved salt in water, ppm/1000000.

Water is divided into four main salinity groups based on amount of dissolved salts in it (Table 3).

Table 3: Salinity level χ of water according to amount of dissolved salts, ppm

Water type	Salinity of water
Fresh water	< 500
Brackish water	500 – 30000
Saline water	30000 – 50000
Brine	> 50000

Acoustic velocity of pure water can also be presented through in-situ pressure and temperature:

$$\begin{aligned} V_{water} &= \sum_{i=0}^{4} \sum_{j=0}^{3} w_{ij} T^i P^j \\ &= 1402.85 + 1.524 \cdot P + 3.437 \times 10^{-3} \cdot P^2 - 1.197 \times 10^{-5} \cdot P^3 + \\ &+ 4.871 \cdot T - 0.0111 \cdot T \cdot P + 1.739 \times 10^{-4} \cdot T \cdot P^2 - 1.628 \times 10^{-6} \cdot T \cdot P^3 - \\ &- 0.04783 \cdot T^2 + 2.747 \times 10^{-4} \cdot T^2 \cdot P - 2.135 \times 10^{-6} \cdot T^2 \cdot P^2 + 1.237 \times 10^{-8} \cdot T^2 \cdot P^3 + \\ &+ 1.487 \times 10^{-4} \cdot T^3 - 6.503 \times 10^{-7} \cdot T^3 \cdot P - 1.455 \times 10^{-8} \cdot T^3 \cdot P^2 + 1.327 \times 10^{-10} \cdot T^3 \cdot P^3 - \\ &- 2.197 \times 10^{-7} \cdot T^4 + 7.987 \times 10^{-10} \cdot T^4 \cdot P + 5.230 \times 10^{-11} \cdot T^4 \cdot P^2 - 4.614 \times 10^{-13} \cdot T^4 \cdot P^3 \end{aligned} \tag{21}$$

Densities of brine and pure water can be approximately computed as follows:

$$\rho_{brine} = \rho_{water} + \chi \cdot (0.668 + 0.44 \cdot \chi + 1\times10^{-6}\left[300 \cdot P - 2400 \cdot P \cdot \chi + T \cdot \left(80 + 3 \cdot T - 3300 \cdot \chi - 13 \cdot P + 47 \cdot P \cdot \chi\right)\right]) \quad (22)$$

$$\rho_{water} = 1 + 1\times10^{-6}(-80 \cdot T - 3.3 \cdot T^2 + 0.00175 \cdot T^3 + 489 \cdot P - 2 \cdot T \cdot P + 0.016 \cdot T^2 \cdot P - 1.3\times10^{-5} \cdot T^3 \cdot P - 0.333 \cdot P^2 - 0.002 \cdot T \cdot P^2) \quad (23)$$

where, ρ_{brine} and ρ_{water} are the densities of brine and pure water respectively, g/cm^3.

After all calculations pressure and temperature dependent bulk modulus of brine water is computed based on the Equation (19).

b) Oil

Elastic properties of bitumen are assumed to be close to properties of heavy oil. Bulk modulus of oil saturated with gas is computed as shown in the Equation (19). P-wave seismic velocity of pseudo live oil at reservoir conditions can be computed as shown below:

$$V_{oil} = 2096\sqrt{\frac{\rho_{oil,sat,pseudo\_rc}}{2.6 - \rho_{oil,sat,pseudo\_rc}}} - 3.7 \cdot T + 4.64 \cdot P + 0.0115 \cdot \left[4.12\sqrt{\frac{1.08}{\rho_{oil,sat,pseudo\_rc}} - 1} - 1\right] \cdot T \cdot P \quad (24)$$

where, $\rho_{oil,sat,pseudo\_rc}$ is the density of synthetic live oil saturated with gas component at simulated reservoir conditions, g/cm^3.

Density of pseudo saturated oil at reservoir conditions can be expressed through density of oil measured at surface conditions (101325 Pa ≈ 0.1 MPa and 15.6 ^{0}C):

$$\rho_{oil,sat,pseudo\_rc} = \frac{\rho_{oil,sc}}{B_0 \cdot (1 + 0.001 \cdot R_G)} \quad (25)$$

where, $\rho_{oil,sc}$ is the density of oil at surface conditions, g/cm^3; B_0 is the oil formation volume factor, which represents ratio of volume of oil and gas at reservoir conditions to volume of oil at surface or standard conditions; R_G is the gas to oil ratio (GOR) or the ratio of gas volume volatilized from saturated oil to volume of the oil at surface conditions, Liters/Liter.

Oil formation volume factor B_0 and GOR R_G can be expressed as shown below:

$$B_0 = 0.972 + 0.00038 \cdot \left[2.4R_G \cdot \left(\frac{G}{\rho_{oil,sc}}\right)^{1/2} + T + 17.8\right]^{1.175} \quad (26)$$

$$R_G = 0.02123 \cdot G \cdot \left[P \cdot \exp\left(\frac{4.072}{\rho_{oil,sc}} - 0.00377 \cdot T\right)\right]^{1.205} \quad (27)$$

where, G is the specific gas gravity or the ratio of the gas density to air density at surface conditions, its value usually varies between 0.56 and 1.80.

The combined effect of pressure, temperature, and gas content on oil density can be expressed as follows:

$$\rho_{oil} = \frac{\rho_{oil,sat,rc} + \left(0.00277 \cdot P - 1.71\times10^{-7} P^3\right)\left(\rho_{oil,sat,rc} - 1.15\right)^2 + 3.49\times10^{-4} P}{0.972 + 3.81\times10^{-4}\left(T + 17.78\right)^{1.175}} \quad (28)$$

where, $\rho_{oil,sat,rc}$ is the density of live oil saturated with gas component at reservoir conditions, g/cm^3.

$$\rho_{oil,sat,rc} = \frac{\rho_{oil,sc} + 0.012 \cdot G \cdot R_G}{B_0} \tag{29}$$

Finally bulk modulus for live oil at reservoir conditions is computed using the Equation 19.

c) Gas

Bulk modulus of hydrocarbon gas can be derived differently as it is done for brine water and saturated oil. Bulk modulus of gas under adiabatic conditions can be expressed as follows:

$$K_{gas} \cong \frac{P}{\left(1 - \frac{P_{pr}}{Z}\frac{\partial Z}{\partial P_{pr}}\right)_T}\gamma \tag{30}$$

where, P_{pr} is the dimensionless pseudoreduced pressure; Z is the compressibility factor (Equation (31)); γ is the heat capacity ratio (ratio of gas heat capacity at constant pressure to gas heat capacity at constant volume), whose expression is shown in the Equation (33).

$$\begin{aligned} Z = &\left[0.03 + 0.00527 \cdot (3.5 - T_{pr})^3\right] \cdot P_{pr} + \left(0.642 \cdot T_{pr} - 0.007 \cdot T_{pr}^4 - 0.52\right) + \\ &+ 0.109 \cdot \left(3.85 - T_{pr}\right)^2 \exp\left\{-\left[0.45 + 8 \cdot \left(0.56 - 1/T_{pr}\right)^2\right] \cdot \frac{P_{pr}^{1.2}}{T_{pr}}\right\} \end{aligned} \tag{31}$$

Thus,

$$\begin{aligned} \left(\frac{\partial Z}{\partial P_{pr}}\right)_{T=T_{pr}} = &0.03 + 0.00527 \cdot \left(3.5 - T_{pr}\right)^3 - \\ &- 0.1308 \cdot \left(3.85 - T_{pr}\right)^2 \frac{P_{pr}^{0.2}}{T_{pr}}\left[0.45 + 8 \cdot \left(0.56 - \frac{1}{T_{pr}}\right)^2\right] \cdot \exp\left\{-\frac{P_{pr}^{1.2}}{T_{pr}}\left[0.45 + 8 \cdot \left(0.56 - \frac{1}{T_{pr}}\right)^2\right]\right\} \end{aligned} \tag{32}$$

$$\gamma = 0.85 + \frac{5.6}{P_{pr} + 2} + \frac{27.1}{\left(P_{pr} + 3.5\right)^2} - 8.7 \cdot \exp\left[-0.65\left(P_{pr} + 1\right)\right] \tag{33}$$

where, T_{pr} is the pseudoreduced temperature, ^{0}C.

Pseudoreduced pressure and temperature can be expressed through absolute pressure P and temperature T of the gas and its specific gravity G:

$$P_{pr} = \frac{P}{P_{pc}} = \frac{P}{4.892 - 0.4048 \cdot G} \tag{34}$$

$$T_{pr} = \frac{T + 273.15}{T_{pc}} = \frac{T + 273.15}{94.72 + 170.75 \cdot G} \tag{35}$$

The density of in-situ gas is calculated as shown below:

$$\rho_{gas} \cong \frac{28.8 \cdot G \cdot P}{Z \cdot R \cdot (T + 273.15)} \tag{36}$$

where, R is the gas constant, 8.314472 J/mol*K.

4. Description of a Program for Generation of Synthetic Seismic Attributes

Description of a parameter file of program `fluidsub_tp.exe` for generation of pressure and temperature dependent synthetic seismic attributes is presented in this section. See the Figure 1 for sample parameter file.

```
                        Parameters for FLUIDSUB_TP
                        **************************

       START OF PARAMETERS:
1-     poro.dat                        -input file with porosity
2-     1                               -   column for attribute
3-     pres.dat                        -input file with pressure in kPa
4-     1                               -   column for attribute
5-     temp.dat                        -input file with temperature in oC
6-     1                               -   column for attribute
7-     wsat.dat                        -input file with brine water saturation
8-     1                               -   column for attribute
9-     osat.dat                        -input file with oil saturation
10-    1                               -   column for attribute
11-    gsat.dat                        -input file with gas saturation
12-    1                               -   column for attribute
13-    1                               -   number of realizations
14-    100     100     100             -   nx, ny, nz
15-    1.580           2.650           -densities of mineral 1 and 2 in g/cm3
16-    0.7                             -volume fraction of mineral 1
17-    15.0            37.0            -bulk moduli of mineral 1 and 2 in GPa
18-    6.0             44.0            -shear moduli of mineral 1 and 2 in GPa
19-    50000.0                         -salinity of brine water in ppm
20-    0.80                            -specific gas gravity G (ratio of gas to air densities)
21-    0.900                           -density of oil at standard (surface) conditions
22-    seismic.out                     -output file for seismic attributes: Vp, Vs, Zp, and Zs
23-    1                               -   standard deviation of measurement error in seismic, %
24-    69069                           -   random number generation seed for measurement error
25-    5      5       5                -   size of smoothing window: nxs, nys, nzs
```

Figure 1: Parameter file of program `fluidsub_tp.exe` for generation of synthetic seismic attributes

After simplification of equations described in previous sections of this paper less number of parameters should be specified for generation of seismic attributes. Static and dynamic properties of a reservoir, mineralogical content and elastic and physical properties of constituent minerals, grid size, and some other miscellaneous parameters should be known to run the program. Names of input files with porosity, reservoir pressure, temperature, brine water, oil and gas saturation values and columns in the files for these attributes are defined on lines 1 to 12. Number of realizations is entered on next line. Number of blocks in a model for all three dimensions is specified on line 14. Densities of constituent two minerals (for instance, clay and quartz) are defined hereafter with volume fraction of first mineral on subsequent line. Elastic bulk and shear moduli of the minerals are specified on lines 17 and 18 respectively. Line 19 is reserved for water salinity. Specific gas gravity (ratio of gas to air densities, which is usually between 0.56 and 1.80) is defined on line 20. Next line is for density of oil at standard or surface conditions (101325 Pa and 16.6 ^{0}C). Name of output file for four seismic attributes are specified on line 22. Generated seismic attributes are P-wave and S-wave seismic velocities, P-wave and S-wave acoustic impedances. Option for addition of measurement, resolution or inversion error to seismic attributes is embedded to the program. The error is just added in from of white noise with zero mean and specified standard deviation in percentage of true value of seismic attribute. Also smoothing window concept can be applied to smooth out values of seismic attributes in adjacent blocks. Both error generation approaches can be combined and applied at the same time as well. All implementation details of the program are presented in the next section through a case study.

5. Case Study

This case study is intended to show which information can be extracted from synthetic seismic attributes, how synthetic seismic attributes can be used in estimation of geological architecture of a reservoir and in prediction of steam chamber growth in SAGD applications, and to present distinction in seismic attribute types. The case study is

built on simplistic oil reservoir model, which characterizes thermal oil recovery process around one SAGD well pair. The model grid is 25 x 25 x 10 blocks of 1.0 m x 1.0 m x 5.0 m size. Block size of a model is larger in Z direction than in any others to account for lower seismic resolution in this direction. The model is schematically shown in the Figure 6 with single well pair, where injector is placed 5 m above producer.

Bitumen extraction rate and steam chamber growth depends on geology of a reservoir, as well as on production scheme. Histograms of true porosity and permeability are shown in the Figure 5. Pressure distribution is derived from porosity values using transform function or probabilistic model, which can be derived from core or log data. Porosity follows normal distribution, while pressure is log normally distributed. Their spatial distribution is presented in the Figure 6. It is assumed that truth is not known and needs to be estimated. From the figures it is obvious that distribution of both porosity and permeability can be divided into two populations. First larger population represents pay zone with good reservoir properties (high porosity and permeability). Sequential Gaussian simulation is used for generation of this population. Second smaller population on the contrary is a representative of flow barrier with poor reservoir properties (low porosity and permeability of single value each). In order to initiate SAGD bitumen recovery process a zone around well pair should be warmed up first to establish communication between the wells. In this case study wells are heated for 90 days and then bitumen production begins. Baseline seismic survey is conducted just before bitumen extraction. Two subsequent seismic surveys are conducted after 90 and 270 days baseline survey is made. Therefore, seismic data are sampled at three time steps: at 0, 90, and 270 days. Generated reservoir pressure and temperature dependent seismic attributes from program `fluidsub_tp.exe` based on Gassmann's fluid substitution model are P- and S-wave seismic velocities and associated P- and S-wave acoustic impedances. All parameters are kept as presented in the sample parameter file (Figure 1). Difference between seismic attributes from baseline survey and all subsequent ones is computed as well using program `seisdif.exe`. The difference is used to diminish presence of geology in prediction of steam chamber growth. True pressure, temperature, water, oil, and gas saturations at three time steps are shown in the Figure 7 – Figure 11 and are obtained from CMG's thermal flow simulator STARS. Note that these reservoir state variables are unknown throughout entire reservoir in real setting, but only at well locations and along well bores. Program `starstogslib.exe` is used to convert STARS' output to GSLib format. Description of parameter files of the programs can be found in the Appendix.

Thus, the objective of the case study is to distinguish between two geological populations (define barrier) and to predict spatial distribution of gas saturation using seismic attributes, and to identify what type of information is inherent in every seismic attribute.

Generated synthetic seismic attributes with no error are shown in the Figure 12 – Figure 19. Open source geomodeling software SGeMS is used to visualize results (Remy et al, 2009). Even though it can be visually detected which attribute can define geology and/or steam chamber, scatter plots with correlation coefficients for porosity and seismic attributes, gas saturation and seismic attributes and their differences are also plotted and used to determine the most informative attribute (Figure 20 - Figure 22 for third time step). It is found that porosity is inversely related to seismic attributes, and gas saturation has negative correlation coefficient with seismic attributes and difference between seismic attributes. The only exception is positive correlation between gas saturation and difference of S-wave velocity, which are directly related. Results are summarized in the Table 4. From the figures and the table it is clear that any seismic attribute can be used to predict barrier (low value porosity region). Steam chamber growth may be predicted poorly by using P-wave velocity, P-wave acoustic impedance and difference of P-wave velocity. However, difference of S-wave velocity and difference of both acoustic impedances can be used to predict steam chamber growth with high accuracy. Linear correlation coefficients and theoretical background of petroelastic model support these findings. Therefore, seismic attribute should be carefully chosen for estimation of specific parameter or state variable of a dynamic reservoir model. For instance, it is better to use S-wave attributes to constrain distribution of porosity. On the other hand difference of S-wave attributes should give fairly good prediction of steam chamber growth. Difference in P-wave acoustic impedance can be used for both porosity estimation and steam chamber growth prediction. Note if error is present in the attributes, the recommendations may change slightly.

Gas saturation and temperature values have same influence on seismic attributes (Figure 23), and, thus, may not be differentiated from each other using seismic attributes. However, reservoir temperature and gas saturation are closely related to each other and have similar spatial distribution in SAGD. And that is why, temperature data can be used to predict steam chamber growth.

Table 4: Prediction ability of synthetic seismic attributes and correlation coefficient

Variable for Estimation	P-wave velocity	S-wave velocity	P-wave acoustic impedance	S-wave acoustic impedance	Δ P-wave velocity	Δ S-wave velocity	Δ P-wave acoustic impedance	Δ S-wave acoustic impedance
Geology (porosity)	Yes -0.959	Yes -0.979	Yes -0.911	Yes -0.991	May be	No	May be	No
Steam chamber (gas saturation)	May be -0.334	No -0.004	May be -0.530	No -0.325	May be -0.498	Yes -0.840	Yes 0.982	Yes -0.979

Influence of measurement, resolution and inverse errors on seismic attributes is examined in this case study as well. Figure 24 shows how P-wave acoustic impedance at second time step changes with increase of error, which is expressed through standard deviation in percentage of true value of the attribute. Figure 25 presents change in P-wave acoustic impedance with decrease of resolution, which is derived from implication of smoothing window concept with specific window size. Combined effect is not shown here, but can be obtained from the program. It is clear that it is getting harder to distinguish between two populations as error and fuzziness go up. Both of them decrease amount of information contained in seismic attributes. Error and fuzziness level should be supported by real data.

6. Conclusion

Methodology for generation of pressure and temperature dependent synthetic seismic attributes based on Gassmann's fluid substitution model is presented in this paper. Program `fluidsub_tp.exe` for proposed petroelastic model is described and case study is presented. Option for error addition is embedded into the program. It is found which seismic attributes can be used for estimation of geology of a reservoir, prediction of steam chamber growth or both. Porosity can be easily detected from seismic; however, permeability should be derived from porosity-permeability relationship. Distribution of gas saturation is tightly related to reservoir temperature in SAGD application, and, thus, temperature data may be used to predict steam chamber growth. In general fluid saturation and reservoir temperature have same effect on seismic attributes and in some cases their combined contribution may not be distinguished. Also amount of information inherent in seismic attributes depends on associated measurement, processing, interpretation errors and resolution (fuzziness) of seismic tools.

References

Batzle, M. and Wang, Z., 1992, Seismic properties of pore fluids, *Geophysics*, 64, 1396-1408

Butler, R., 1991, *Thermal Recovery of Oil and Bitumen*, Prentice Hall, Englewood Cliffs, New Jersey, 524 pp.

Deutsch, C.V. and Journel, A.G., 1998, *GSLIB: Geostatistical Software Library and User's Guide*, Oxford University Press, New York, 2nd Ed., 369 pp.

Fahimuddin, A., 2010, 4D Seismic History Matching Using the Ensemble Kalman Filter (EnKF): Possibilities and Challenges, *PhD Thesis*, University of Bergen, Norway, 116 pp.

Gassmann, F., 1951, Über die elastizität poröser medien: Vierteljahrsschrift der Naturforschenden Gesellschaft in Zurich, 96, 1-23. The English translation of this paper is available at http://sepwww.stanford.edu/sep/berryman/PS/gassmann.pdf

Hong, S. and Deutsch, C., 2008, Fluid Substitution Model to Generate Synthetic Seismic Attributes: `FluidSub.exe`, *Centre for Computational Geostatistics* 10, 204-1 – 204-8

Hong, S., Leuangthong, O. and Deutsch, C., 2006, A Geostatistical Approach to Stochastic Seismic Inversion, *Centre for Computational Geostatistics* 8, 201-1 – 201-22

Krief, M., Garat, J., Stellingwerff, J. and Ventre, J., 1990, A Petrophysical Interpretation Using the Velocities of P and S Waves (Full-Waveform Sonic), *The Log Analyst*, 355-369

Kumar, D., 2006, A Tutorial on Gassmann Fluid Substitution: Formulation, Algorithm and Matlab Code, *Geohorizons*, p 4-12

Lumley, D., 2001, Time-Lapse Seismic Reservoir Monitoring, *Geophysics*, Vol. 66, No 1, p. 50 – 53

Mavko, G., Mukerji, T. and Dvorkin, J., 2009, *The Rock Physics Handbook: Tools for Seismic Analysis in Porous Media*, Second Edition, Cambridge University Press, New York, 525 pp.

Remy, N., Boucher, A. and Wu, J., 2009, *Applied Geostatistics with SGeMS: A User's Guide*, Cambridge University Press, New York, 264 pp.

Zhang, W., Youn, S. and Doan, Q., 2005, Understanding Reservoir Architectures and Steam Chamber Growth at Christina Lake, Alberta, by Using 4D Seismic and Croswell Seismic Imaging, *SPE/PS-CIM/CHOA International Thermal Operations and Heavy Oil Symposium*

Appendix

Description of parameter files of two simple, but vital programs `starstogslib.exe` and `seisdif.exe` is given in this Appendix.

a) Description of a Program to Convert STARS' Output to GSLib Format

This program transforms output of CMG's thermal flow simulator STARS to GSLib format (Deutsch and Journel, 1998). Description of the parameter file can be found in the Figure 2. STARS's output is specified on first line. Then number of blocks in model grid for three dimensions is defined. Model may have two or three dimensions. Number of time steps, for which data should be transformed, is entered on line 3. Next line is used to determine time steps in days for data extraction. Name for output file, which contains reservoir pressure, temperature, water, oil, and gas saturations, is defined on last 5th line. Error messages may show up, if something wrong occurs in calculation procedure, format of STARS' output file is not set up properly or input file is missing.

```
                        Parameters for STARStoGSLib
                        ***************************
      START OF PARAMETERS:
1-    stars.out                       -input file with STARS simulation results
2-    100     100     100             -   nx, ny, nz
3-    3                               -how many times should data be extracted?
4-    120.0   240.0   360.0           -   time for extraction, days
5-    stars_gslib.out                 -output file for simulation results
```

Figure 2: Parameter file of `starstogslib.exe` program for converting STARS's output to GSLib format

b) Description of a Program to Compute Change in Seismic Attributes with Time

This program is designed to compute difference between seismic attributes from baseline seismic survey and any other subsequent surveys. File name with attributes from baseline survey and column for required attribute are specified on lines 1 and 2 respectively. Number of follow-up surveys $N_{follow\text{-}up}$ is entered on line 3. Next $2*N_{follow\text{-}up}$ lines are dedicated for file names with follow-up seismic attributes and columns for relevant data. Output file name, which contains difference of seismic attributes (seismic from i^{th} follow-up seismic survey minus seismic from baseline survey), is defied on last line.

```
                        Parameters for SEISDIF
                        **********************
      START OF PARAMETERS:
1-    base_survey.out                 -input file with seismic attributes from base survey
2-    1                               -   column for attribute
3-    2                               -number of follow-up surveys
4-    1_survey.out                    -input file with seismic attributes from 1st survey
5-    1                               -   column for attribute
6-    2_survey.out                    -input file with seismic attributes from 2nd survey
7-    1                               -   column for attribute
8-    seisdif.out                     -output file for difference between seismic attributes
```

Figure 3: Parameter file of `seisdif.exe` program for computing difference of seismic attributes

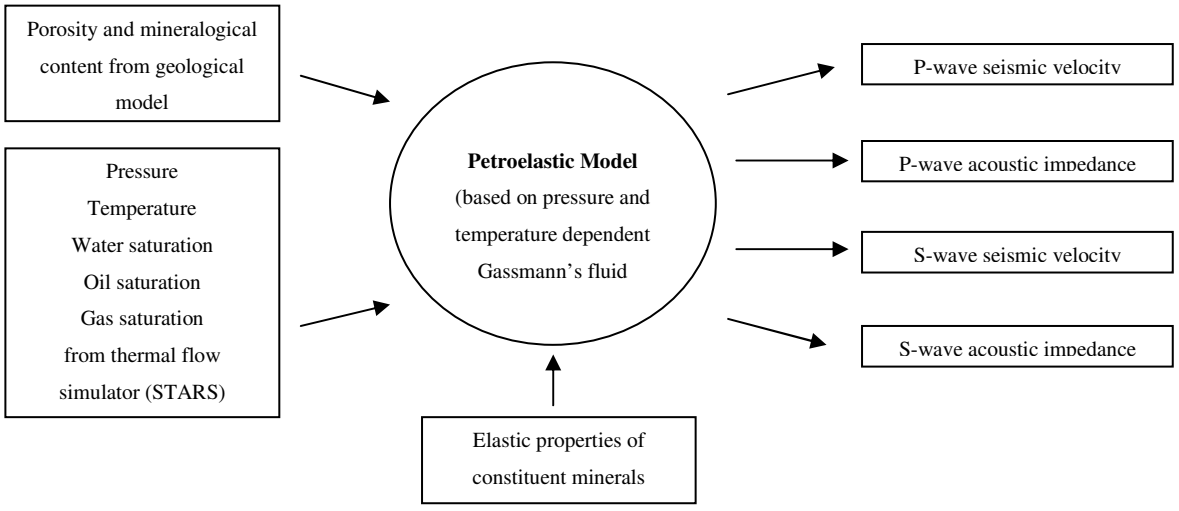

Figure 4: Schematic of petroelastic model based on Gassmann's fluid substitution model used for generation of pressure and temperature dependent seismic attributes

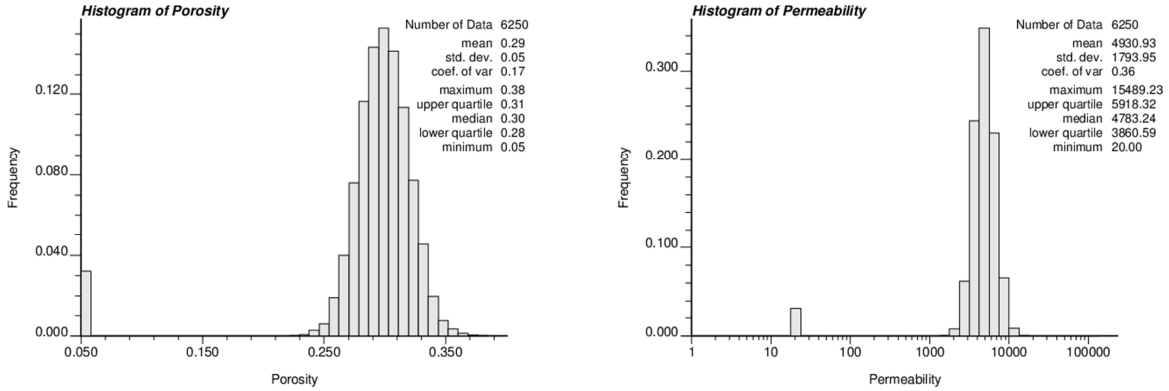

Figure 5: Histograms of porosity and permeability

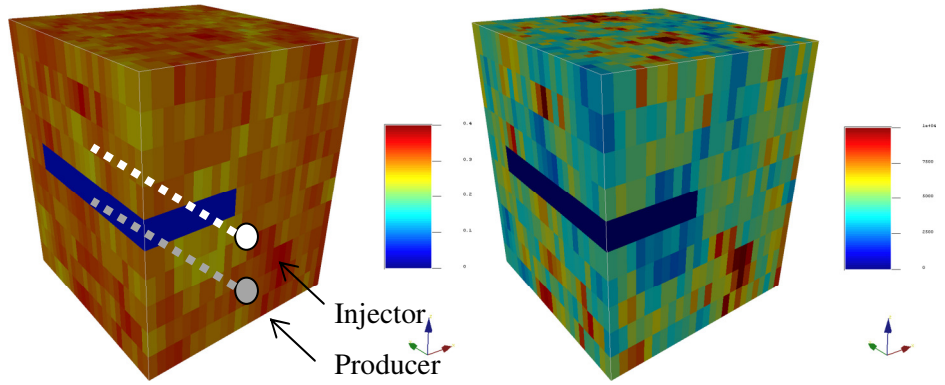

Figure 6: Porosity and permeability models. SAGD well pair goes through middle-bottom section along Y axis

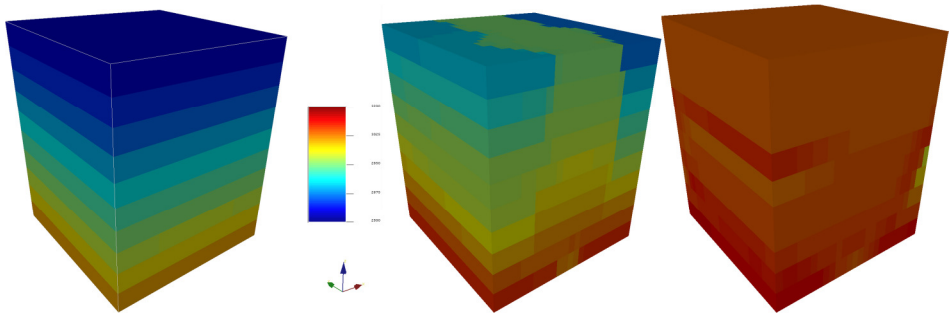

Figure 7: Pressure distribution at the beginning of bitumen extraction (0 days) and after 90 and 270 days

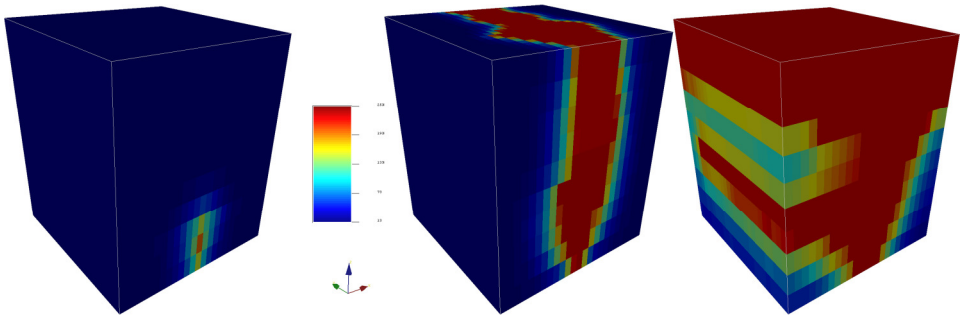

Figure 8: Temperature distribution at the beginning of bitumen extraction (0 days) and after 90 and 270 days

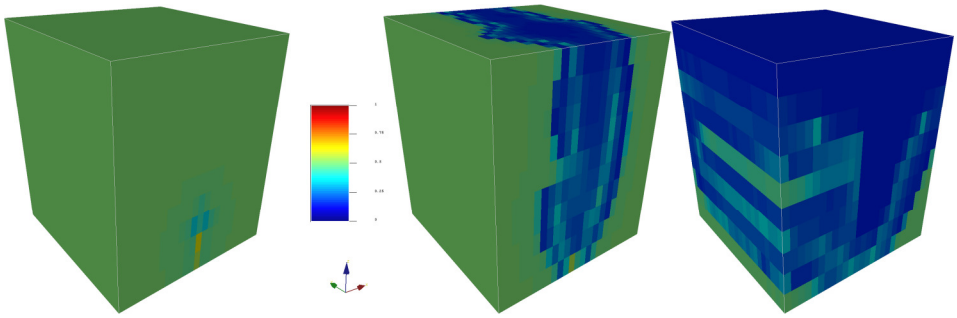

Figure 9: Brine water saturation at the beginning of bitumen extraction (0 days) and after 90 and 270 days

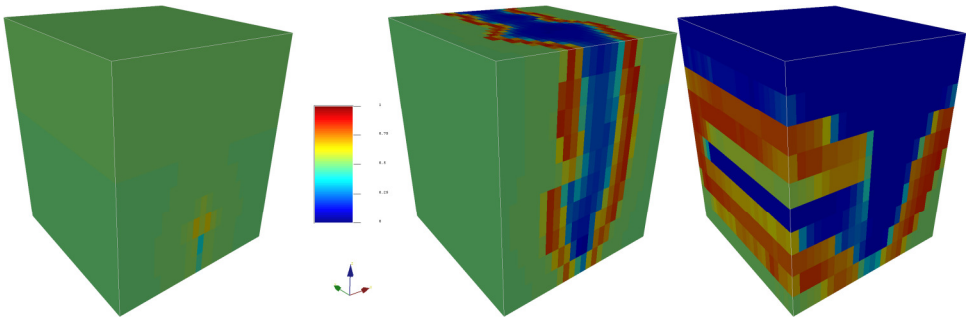

Figure 10: Oil saturation at the beginning of bitumen extraction (0 days) and after 90 and 270 days

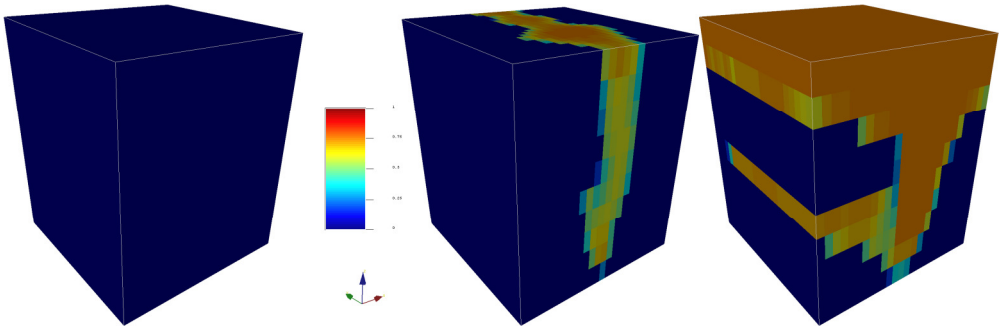

Figure 11: Gas saturation at the beginning of bitumen extraction (0 days) and after 90 and 270 days

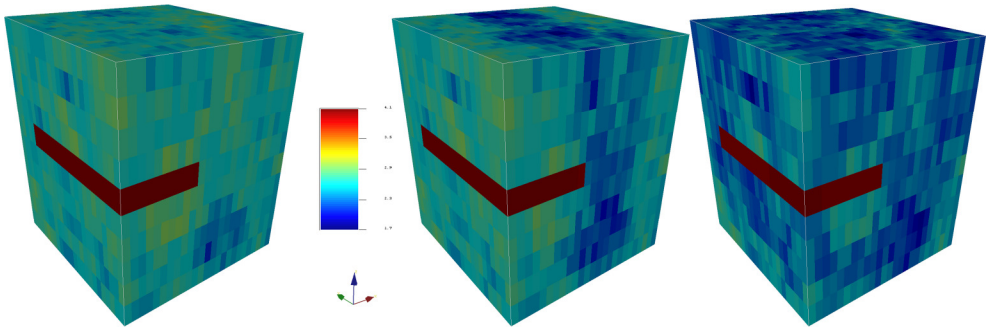

Figure 12: P-wave velocity distribution at the beginning of bitumen extraction (0 days) and after 90 and 270 days

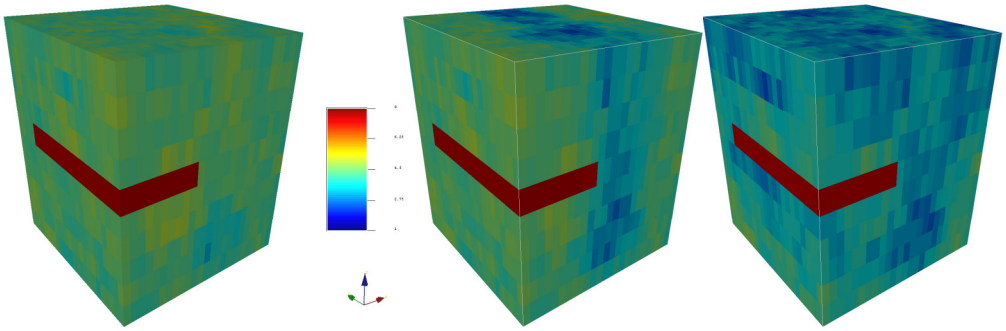

Figure 13: P-wave acoustic impedance distribution at the beginning of bitumen extraction (0 days) and after 90 and 270 days

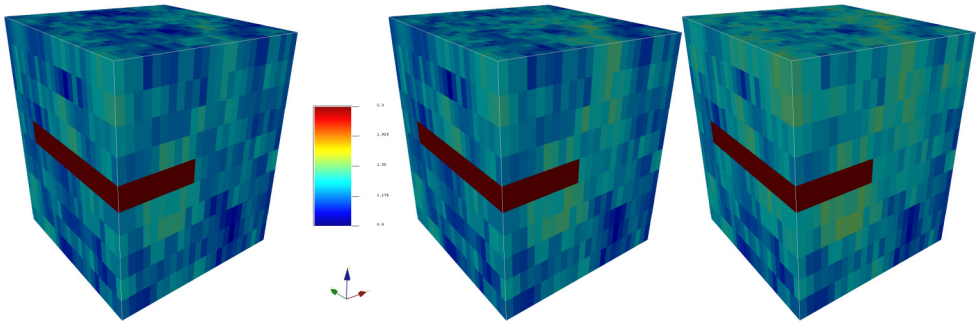

Figure 14: S-wave velocity distribution at the beginning of bitumen extraction (0 days) and after 90 and 270 days

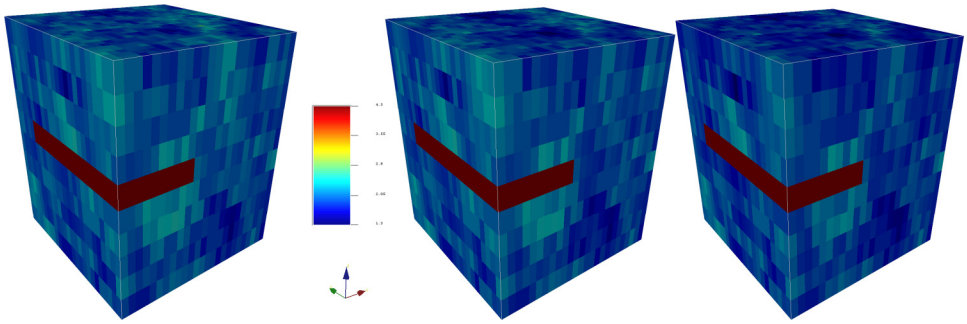

Figure 15: S-wave acoustic impedance distribution at the beginning of bitumen extraction (0 days) and after 90 and 270 days

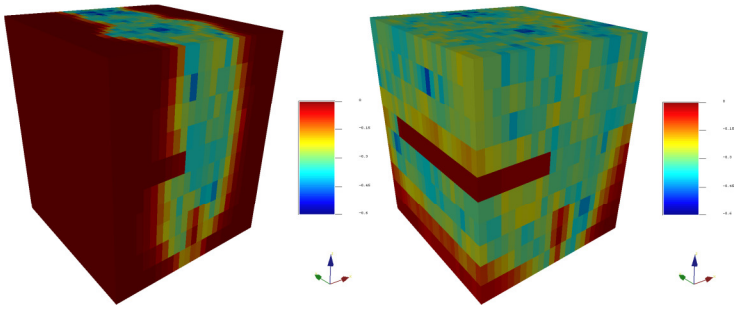

Figure 16: Difference of P-wave velocity: P-velocity from survey after 90 days – P-velocity from base survey (left), P-velocity from survey after 270 days – P-velocity from base survey (right)

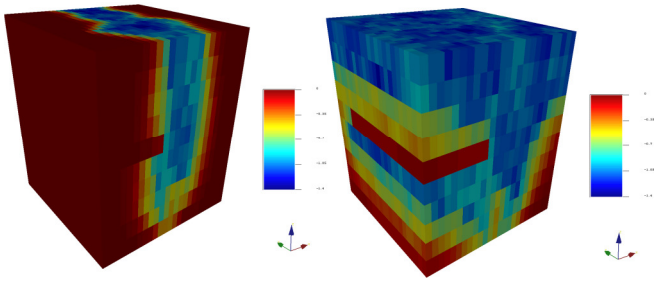

Figure 17: Difference of P-acoustic impedance: P-Z from survey after 90 days – P-Z from base survey (left), P-Z from survey after 270 days – P-Z from base survey (right)

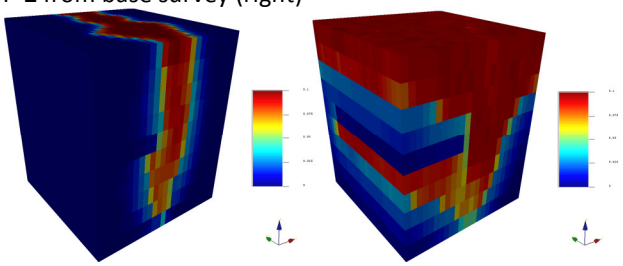

Figure 18: Difference of S-wave velocity: S-velocity from survey after 90 days – S-velocity from base survey (left), S-velocity from survey after 270 days – S-velocity from base survey (right)

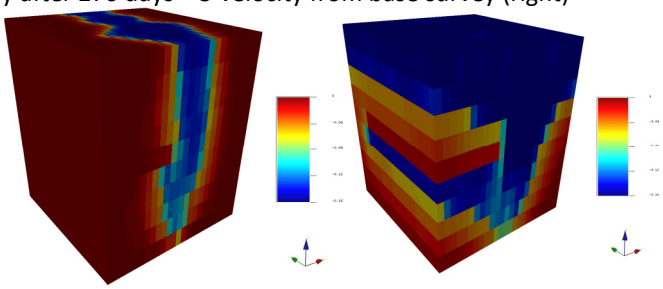

Figure 19: Difference of S-acoustic impedance: S-Z from survey after 90 days – S-Z from base survey (left), S-Z from survey after 270 days – S-Z from base survey (right)

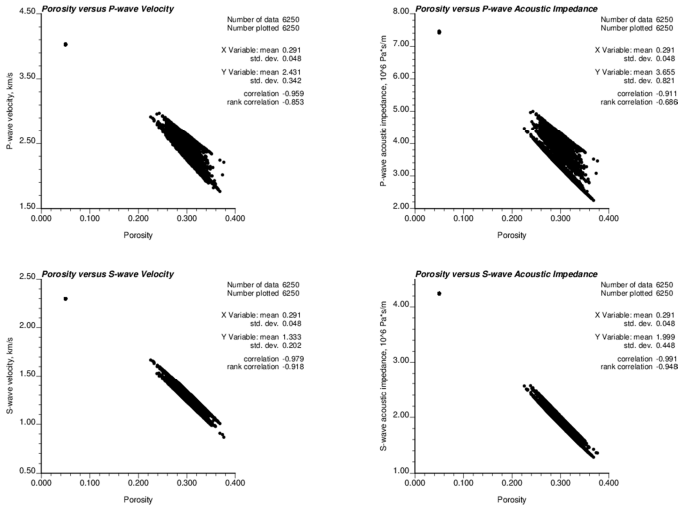

Figure 20: Scatter plots of porosity versus seismic velocities and acoustic impedances after 270 days of bitumen extraction

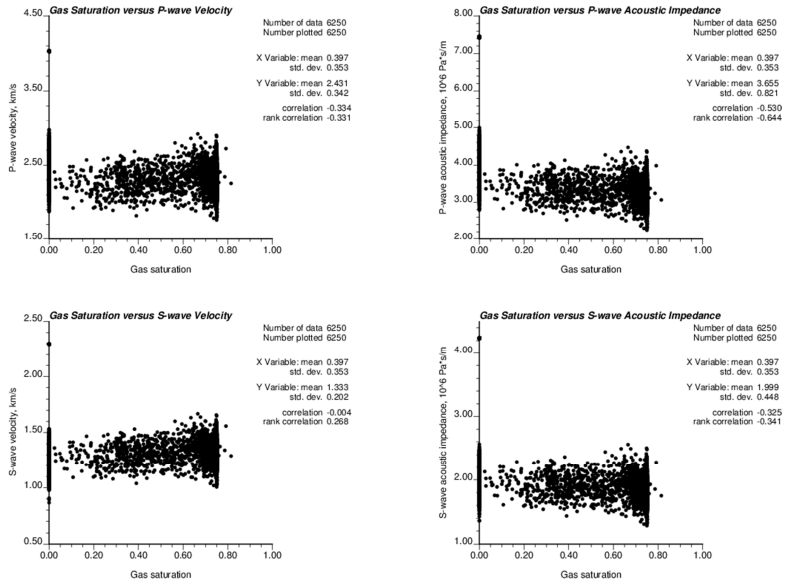

Figure 21: Scatter plots of gas saturation versus seismic velocities and acoustic impedances after 270 days of bitumen extraction

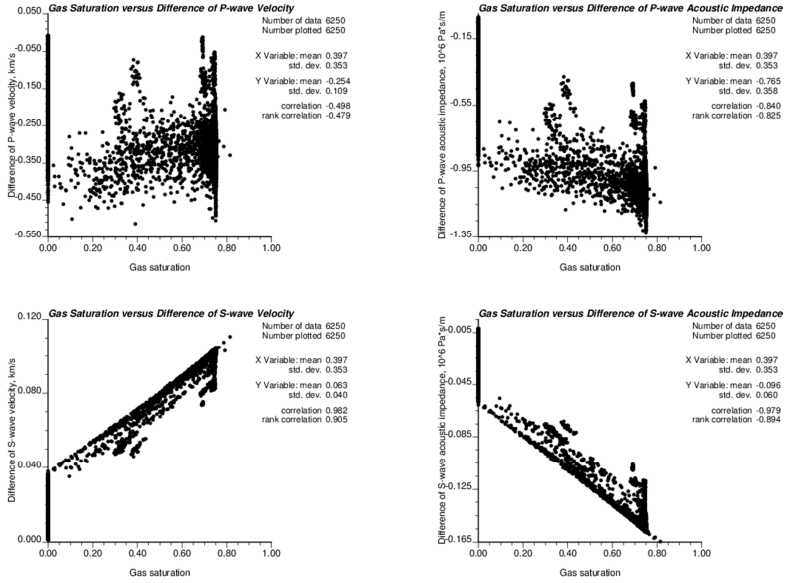

Figure 22: Scatter plots of gas saturation versus difference of seismic velocities and acoustic impedances between beginning and after 270 days of bitumen extraction

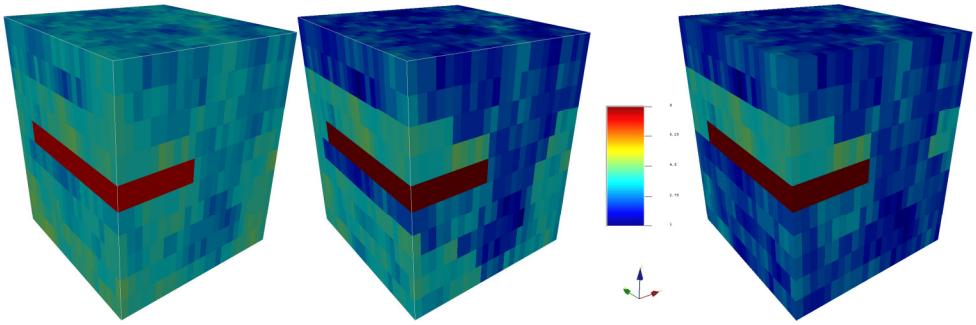

Figure 23: Influence of temperature versus fluid type on P-wave acoustic impedance (270 days): temperature varies in space (left), temperature is low and constant (middle), temperature is bimodal – high below barrier and low above it (right)

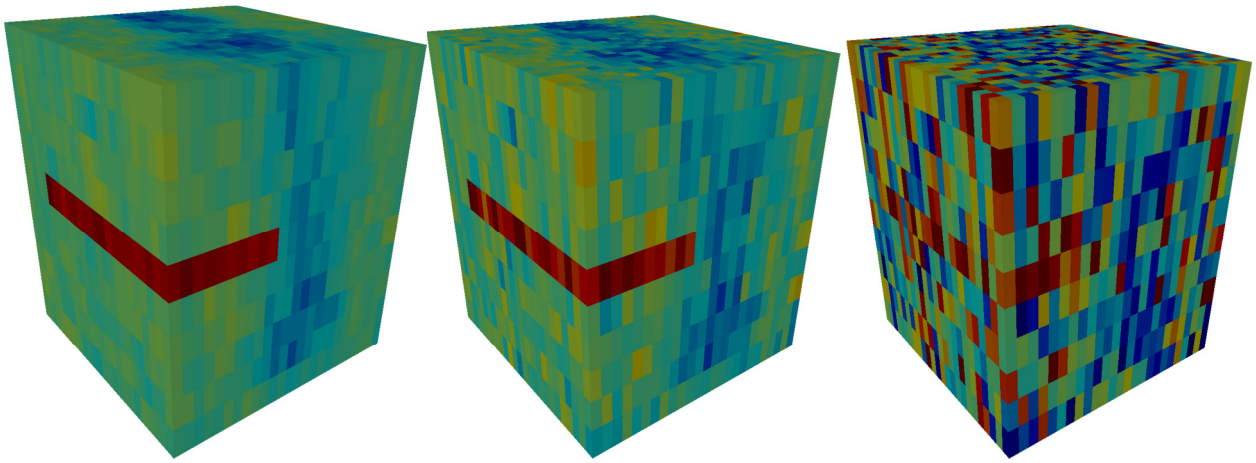

Figure 24: Influence of measurement error on seismic attributes (P-wave acoustic impedance after 90 days of extraction): standard deviation of measurement error is 1% of true value, 5% and 20%

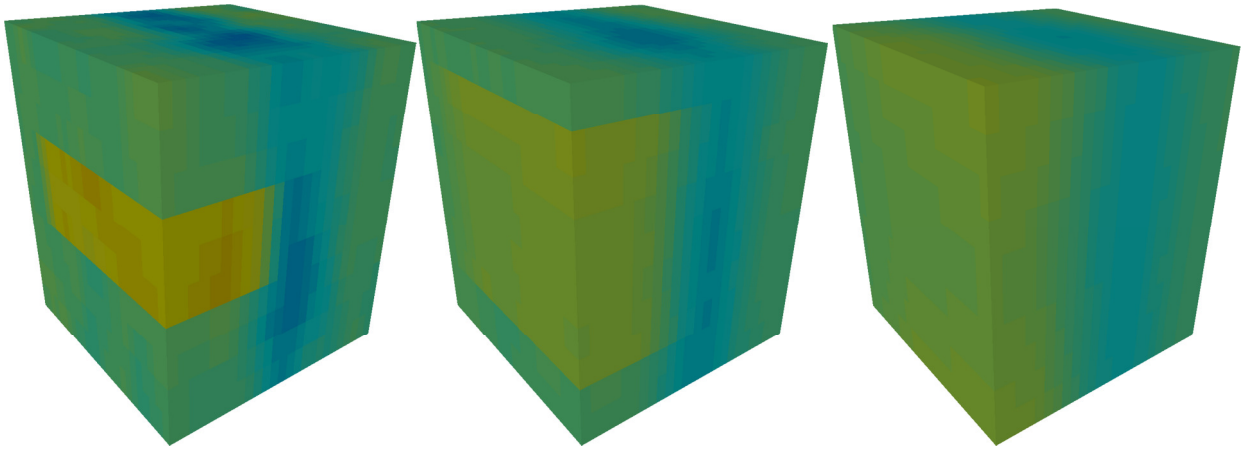

Figure 25: Influence of smoothing effect on seismic attributes (P-wave acoustic impedance after 90 days of extraction): smoothing window size is 1 block, 3 blocks and 5 blocks